HIGH TEMPERATURE THERMAL PROPERTIES OF MAGNESIUM SILICIDE INVESTIGATED BY MOLECULAR DYNAMICS SIMULATION

Meena Rittiruam[a,b,*], Keerati Maneesai[c], Korakot Matarat[a,d], Athorn Vora-ud[b], Sirakan Yokhasing[a,b]

[a]*Simulation Research Laboratory, Center of Excellence on Alternative Energy, Research and Development Institution, Sakon Nakhon Rajabhat University, Sakon Nakhon, 47000, Thailand*
[b]*Program of Physics, Faculty of Science and Technology, Sakon Nakhon Rajabhat University, Sakon Nakhon, 47000, Thailand*
[c]*Faculty of Science and Engineering, Kasetsart University Chalermphrakiat Sakonnakhon Province Campus, Sakon Nakhon, 47000, Thailand*
[d]*Program of Computer, Faculty of Science and Technology, Sakon Nakhon Rajabhat University, Sakon Nakhon, 47000, Thailand*

Received 15 January 2017; Revised 15 May 2017; Accepted 5 June 2017

ABSTRACT

The thermal properties are important for processing conversation heat energy to electricity of Magnesium Silicide (Mg_2Si) thermoelectric material. This work, we investigate the thermal properties of Mg_2Si by using molecular dynamics (MD) simulation. The cluster atomic model was designed by using $Mg_{512}Si_{256}$ based on CaF_2 structure for MD calculation. The Morse-type and Busing-Ida type were performed for inter-atomic interaction based on MXDORTO. Our calculated results composed lattice parameter, compressibility, linear thermal expansion coefficient, energy, heat capacity, and thermal conductivity, respectively, they present at versus temperature 300 – 1200 K. In addition, the heat flux auto-correlation and thermal conductivity depend on time correlation was presented. The calculated imply that the thermal conductivity of Mg_2Si become to ~1 W m^{-1} K^{-1} at high temperature.

KEYWORDS: *Thermal conductivity; Green-Kubo relation; Heat capacity; MXDORTO*

* Corresponding authors; e-mail: meena@snru.ac.th ,Tel&Fax: +664-274-4319

INTRODUCTION

Magnesium silicide is a non-toxicity thermoelectric (TE) material [1]. General, it exhibits n-type TE material. Whereas, the Bi-, Sb- and Al-doping lead to p-type TE material [2]. In addition, the Mg_2Si is intermediated thermoelectric power generator at high temperature applications with maximum operating temperature of around 600 K [3]. So far, the structural behaviors of Mg_2Si have been investigated by energy dispersive synchrotron X-ray diffraction. It was found that, the crystal structure of Mg_2Si is anti-fluorite (CaF_2) type (Pearson symbol; *cF*12, space group symbol; *Fm3m* and space group number; 225) with lattice parameter of 0.635 nm and density of 1.90 g cm^{-3} [4–6]. As well know, the Mg_2Si exhibits low thermal conductivity at room to middle temperature [7–9]. In addition, the experimental shows the heat capacity at constant volume is 67.6 J mol^{-1} K^{-1} [10], heat capacity at constant pressure is 67.9 J mol^{-1} K^{-1} [10], and thermal conductivity 5.2 – 10.5 W m^{-1} K^{-1} [11, 12] at room temperature, respectively. However, the thermal properties such as lattice parameter, compressibility, linear thermal expansion coefficient, internal energy, heat capacity, and thermal conductivity at high temperature is a few reported. This work, we investigated the thermal properties of Mg_2Si. This presents are help to understand behavior of TE as well as future applications at high temperature.

MATERIALS AND METHODS

Computational details

The MD calculation on thermal properties of Mg_2Si was performed using the system of 768 ions that composed Mg (cations) 512 ions, and Si

Table 1 The conditions for MD calculation of Mg_2Si

Calculation	L, B, α_{lin}	C_P, C_V, C_d	κ
System			
-Particles	768 Particles (512 cations and 256 anions)		
	Mg = 512, Si = 256		
-Structure	CaF_2 crystal structure		
Control			
-Temperature	Scaling method	Scaling method	Nose method [14]
-Pressure	Scaling method	No control method	Andersen method [15]
Number of steps	100,000	100,000	100,000

Table 2 The inter-atomic potential parameter for Mg_2Si

Ions	z	a	b	c		D_{ij}	β_{ij}	r_{ij}^*
Mg	1.2	1.926	0.11405	20	Pair Mg–Si	15	2.25	2.369
Si	–2.4	1.659	0.11405	0				

(anions) 256 ions in dimension 4×4×4 unit cells. The cluster atom model was initially arranged in the CaF_2 type crystal structure as shown in Fig. 1. The calculation conditions of the lattice parameter (L), compressibility (B), linear thermal expansion coefficient (α_{lin}), heat capacity at constant pressure (C_P), heat capacity at constant volume (C_V), heat capacity of lattice dilatational terms (C_d), and thermal conductivity (κ) as shown in Table 1. This calculation was performed by MXDORTO [13].

The Morse-type [16] and Busing-Ida type [17] potential function were employed for inter-atomic interaction, as show in equation. (1).

$$U_{ij}(r_{ij}) = \frac{z_i z_j e^2}{r_{ij}} + f_0(b_i + b_j)\exp\left(\frac{a_i + a_j - r_{ij}}{b_i + b_j}\right) - \frac{c_i c_j}{r_{ij}^6} + D_{ij}\left\{\exp\left[-2\beta_{ij}(r_{ij} - r_{ij}^*)\right] - 2\exp\left[-\beta_{ij}(r_{ij} - r_{ij}^*)\right]\right\} \quad (1)$$

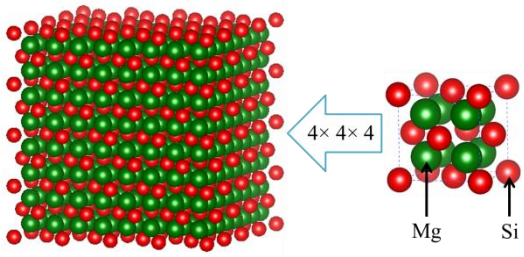

Fig. 1 The $Mg_{512}Si_{256}$ cluster atoms model for Mg_2Si 4×4×4 unit cells.

Here, f_0 is repulsion between atoms in vacuum (4.186), z_i and z_j are the effective partial electronic charges on the i^{th} and j^{th} ions, respectively. r_{ij} is the inter-atomic distance, r_{ij}^* is the bond length of the cation-anion pair in vacuum. The parameters of *a*, *b* and *c* are the characteristic parameters depending on the ion species. The potential function, D_{ij} and β_{ij} describe the depth and shape of this potential, respectively. The first term describes the Coulomb interactions and the second term denotes core repulsions. The third term is a Morsetype potential, and applied only to cation-anion pairs. The values of the inter-atomic potential parameters used in the present study are given in Table 2.

The calculations were performed on cluster computer, OS-Rocks Clusters 6.1.1 (based on Centos 6.5) 64 bit, total 6 cores (Intel ® Core(TM) 2 Quad CPU Q9500 @ 2.83GHz 2.83 GHz) and total 8 GB of RAM.

RESULTS AND DISCUSSION

The L of Mg_2Si carried out by MD calculation at pressure 0.1 MPa and temperature 300 – 1200 K as shown in Fig. 2. Our calculated L with value of a = b = c = 6.3516±0.0004 Å at room temperature show good agreement with the experimental data [6, 18, 19]. It was note that, the structure of Mg_2Si was expanded with increasing temperature. Our calculated of L show a few error

at high temperature and denote that high accurate of MD. In addition, L was adopted to investigate the B and α_{lin} following by equations. (2) and (3);

$$B = \frac{3}{L(\mathrm{P}_0)}\left(\frac{\partial L(\mathrm{P})}{\partial P}\right)_{\mathrm{T}} \tag{2}$$

$$\alpha_{\text{lin}} = \frac{1}{L(\mathrm{T}_0)}\left(\frac{L(\mathrm{T})-L(\mathrm{T}_0)}{T-T_0}\right)_{\mathrm{P}} \tag{3}$$

Here, $L(\mathrm{P})$, P_0, $L(\mathrm{T})$, and T_0 are L at pressure $P(\mathrm{Pa})$, atmospheric pressure, the L at $T(\mathrm{K})$ and room temperature, respectively. The calculated of B and α_{lin} as show in Fig. 3.

Our calculated of B exhibits value 6.2 MPa^{-1} at 300 K slowly increase to 7.65 MPa^{-1} at 1200 K. Meanwhile, the α_{lin} exhibits 8.6 $\mu\mathrm{K}^{-1}$ at 350 K increase like exponential function to 10.48 $\mu\mathrm{K}^{-1}$ at 1200 K. These results help to understand and confirm that the structure of Mg_2Si has expanded as exponential function and affect to the heat capacity and thermal conductivity.

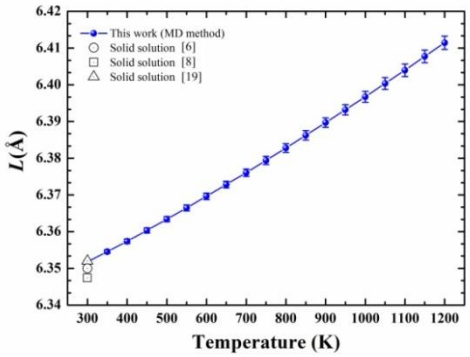

Fig. 2 Calculated of lattice parameters for Mg_2Si at various temperatures.

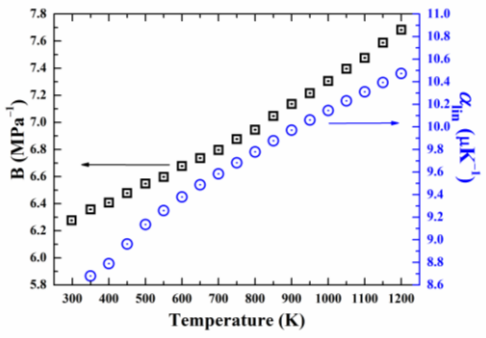

Fig. 3 Calculated of compressibility and linear thermal expansion coefficient for Mg_2Si at various temperatures.

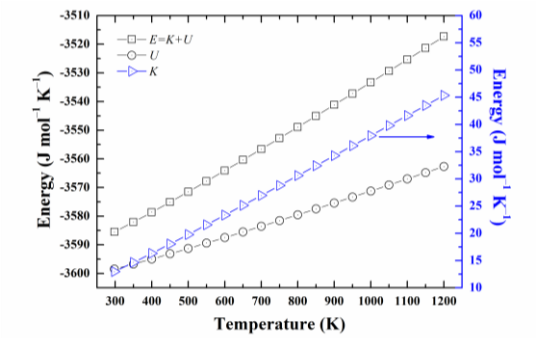

Fig. 4 Calculated of internal energy of Mg_2Si at various temperatures.

The kinetic energy (K), potential energy (U) and total energy (E) were directly carried out by MD calculation can evaluate by equations. (4) – (6);

$$E = U + K \tag{4}$$

$$\begin{aligned} U &= U_{\text{Coulomb}} + U_{\text{short}} \\ &= U_{\text{Coulomb}} + U_{\text{vdW}} + U_{\text{srr}} + U_{\text{Morse}} \end{aligned} \tag{5}$$

$$K = \frac{1}{3Nk_{\mathrm{B}}}\sum_i m_i v_i^2 \tag{6}$$

Here, U_{Coulomb}, U_{vdW}, U_{srr}, U_{Morse} N, k_{B}, m_i and v_i are Coulomb potential, van der Waals attraction, short range repulsion, Morse potential energy, number of atom, Boltzmann constant, mass of atom i and, velocity of atom i, respectively, Our calculated of internal energy for Mg_2Si as shown in Fig. 4.

The C_{p} can evaluated by $C_{\mathrm{V}} + C_{\mathrm{d}}$; where C_{V} regards to gradient of the total internal energy and C_{d} can evaluated by using L, B, and α_{lin} as following in equations. (7) – (9);

$$C_{\mathrm{P}} = C_{\mathrm{V}} + C_{\mathrm{d}} \tag{7}$$

$$C_{\mathrm{V}} = \left(\frac{\partial E(\mathrm{T})}{\partial T}\right)_{\mathrm{V}} \tag{8}$$

$$C_{\mathrm{d}} = \frac{(3\alpha_{\text{lin}})^2 V_m(\mathrm{T})}{B}T \tag{9}$$

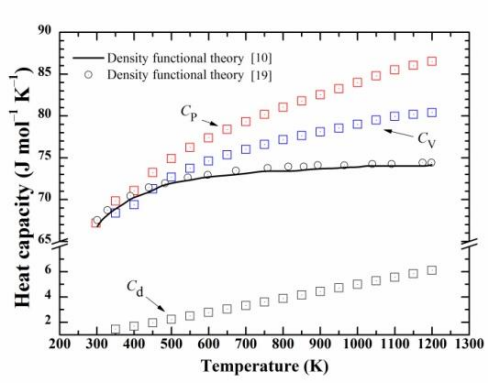

Fig. 5 Calculated of heat capacity of Mg_2Si at various temperature.

Here $V_m(\mathrm{T})$ is the molar volume at temperature $T(\mathrm{K})$. Our calculated of C_d show a few value about of 1.4 J mol^{-1} K^{-1} at 300 K increased to 6.1 J mol^{-1} K^{-1} at 1200 K. It denote that perturbation term of lattice vibration. Our calculated of C_V show agree with experimental data of Wang [10] at 350 – 500 K. It slightly increases above 500 K. The C_P and C_V were began constant above 1100 K thus agree with Dulong-Pertit law. Our calculated of C_P show agreement values with experimental data at 300 – 450 K, while more than experimental data above 450 K [19].

The lattice thermal conductivity can be investigated by using the Green-Kubo relation [20]. It obtained from time integral of heat flux auto-correlation function (ACF) of the energy current as following by equation. (10) – (12);

$$\kappa_{\mathrm{lat}} = \frac{R}{3N_\mathrm{A}T^2}[L(\mathrm{T})]^3 \int_0^\infty \langle S(\mathrm{t})S(0)\rangle \mathrm{d}t \qquad (10)$$

$$S(\mathrm{t}) = \frac{1}{[L(\mathrm{T})]^3}\left[\sum_j E_j v_j + \frac{1}{2}\sum_j\sum_{i\neq j} r_{ij}(f_{ij}v_j)\right] \qquad (11)$$

$$E_j = \left\{\frac{1}{2}m_j v_j^2 + \frac{1}{2}\sum_{i\neq j} U_{ij}(r_{ij})\right\} - E_{\mathrm{av}} \qquad (12)$$

where R, N_A, $S(t)$, t, m_j, v_j, f_{ij}, E_j and E_{av} are the gas constants = 8.314 J K^{-1} mol^{-1}, Avogadro constant, the heat flux form auto–correlation function (ACF), time correlation, mass of atom *j*, velocity of atom *j*, force between atom *i* and *j*; energy of atom *j* and average energy of the system, respectively.

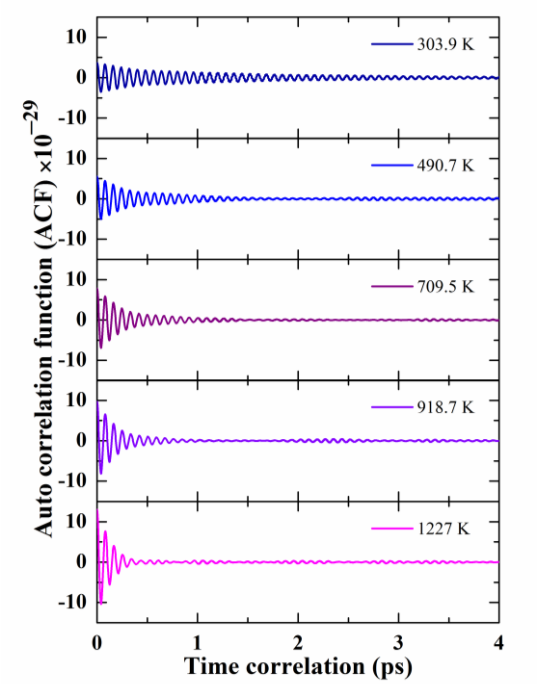

Fig. 6 The calculated of auto-correlation function for Mg_2Si at versus time correlation.

The expectation of auto-correlation function, $\langle S(\mathrm{t})S(0)\rangle$, and calculated of κ_{lat} for Mg_2Si as shown in Fig. 6 and 7. The ACF take approximately 4.0 ps and decay to zero, while the κ_{lat} has value about 8.48 W m^{-1} K^{-1} at 4.0 ps, which occurred at at 303.9 K. It should be that, the ACF and κ_{lat} has been quick decay to zero where increasing temperature. In addition, the ACF is direct variation of temperature while κ_{lat} opposite.

The thermal conductivity of Mg_2Si at versus temperature as shown in Fig. 8. Our calculated of κ_{lat} exhibits 8.48 W m^{-1} K^{-1} at 303.9 K decreased to 1.52 W m^{-1} K^{-1} at 1227 K. We using the calculation result of κ_{lat} compared with literature data thus composed many method such as, solid state reaction (SSR) [11, 12, 21, 22], spark plasma sintering (SPS) [23, 24], plasma activated sintering (PAS) [25, 26] and field-activated and pressure-assisted synthesis (FAPAS) [27].

All literatures exhibit the total thermal conductivity which can evaluate by $\kappa = \kappa_{\mathrm{lat}} + \kappa_e$, here κ_e is electron thermal conductivity term. While, the MD calculation carried out the lattice thermal conductivity which

less than experimental data [11, 21, 23 – 27] and more than of experimental data [12, 22]. It indicate that good TE property, because of good TE materials are required low thermal conductivity [1, 3]. Moreover, we present the κ_{lat} above 900 K shown slightly decrease to 1 W m^{-1} K^{-1}. Our calculated of thermal conductivity can be predicted by equation (13);

$$\kappa_{lat}[\mathrm{W\,m^{-1}\,K^{-1}}] = \kappa_0 + 23.8\exp[-0.004T(\mathrm{K})];\quad \kappa_0 = 1.53 \tag{13}$$

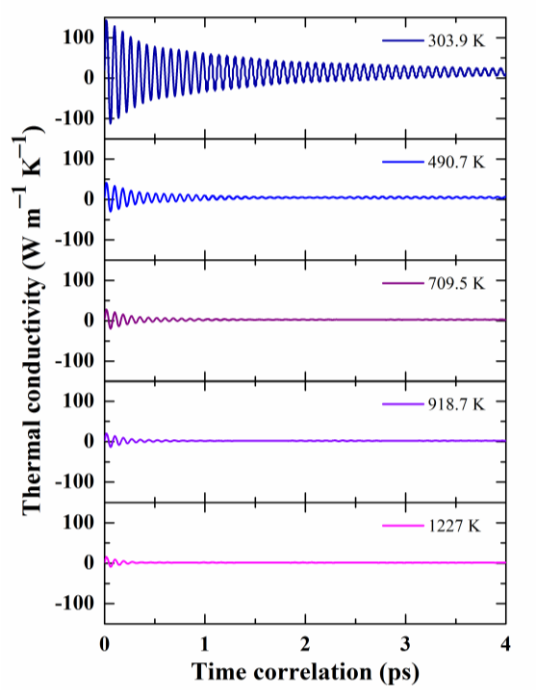

Fig. 7 The calculated of lattice thermal conductivity for Mg_2Si at versus time correlation.

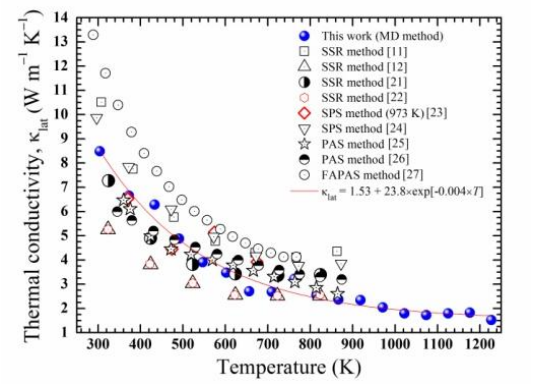

Fig. 8 The calculated of lattice thermal conductivity together with literature data at various temperature.

CONCLUSION

The thermal properties composed L, B, α_{lin}, C_P, C_V, C_d, ACF, and κ_{lat} of Mg_2Si has been successfully investigated by MD simulation. The L, B and α_{lin} indicated that structure of Mg_2Si is expansion and contraction as exponential function as well as contribute to C_P, C_V, C_d, and κ_{lat} also change as exponential function. Our calculated of κ_{lat} estimated that the κ_{lat} decreased to 1 W m^{-1} K^{-1} at high temperature.

ACKNOWLEDGEMENTS

This work was supported by Thailand Research Fund (TRF) through the Royal Golden Jubilee (RGJ) Ph.D. Program (Grant No. PHD/0195/2558).

REFERENCES

[1] S. Fiameni, S. Battiston, S. Boldrini, A. Famengo, F. Agresti, S. Barison, M. Fabrizio, Synthesis and characterization of Bi-doped Mg_2Si thermoelectric materials. J. Solid. State. Chem. 193 (2012) 142–146.

[2] D.M. Rowe, G. Min, Multiple potential barriers as a possible mechanism to increase the Seebeck coefficient and electrical power factor. 13th Int. Conf. on thermoelectrics, New York. 30 August – 1 September 1994, 339–342.

[3] R. Saravanana, M.C. Robert, Local structure of the thermoelectric material Mg_2Si using XRD, J. Alloy. Compd. 479 (2009) 26–31.

[4] H.K. Mao, J. Xu, P.M. Bell, Calibration of the ruby pressure gauge to 800 kbar under quasi-hydrostatic conditions, J. Geophys. Res. 91 (1986) 4673–4676.

[5] J. Hao, B. Zou, P.W. Zhu, C.X. Gao, Y.W. Li, D. Liu, K. Wang, W.W. Lei, Q.L. Cui, G.T. Zou, In situ X-ray observation of phase transitions in under high pressure, Solid. State. Commun. 149 (2009) 689–692.

[6] E.N. Nikitin, A.I. Zaslavskii, A.K. Kusnetsov, V.K. Zaitsev, E.N Tkalenko, A study of the phase diagram for the Mg_2Si-Mg_2Sn system and the properties of certain of its solid solutions, J. Inorganic Mater. 4 (1968) 1656–1659.

[7] M. Umemoto, Y. Shirai, K. Tsuchiya, The 4th Pacific Rim Int. In Conf. on Advanced Materials and Processing (PRICM4), S. Handa and Z. Zhong (Eds), SW Nam and RN Wright, (Jpn. Inst. Met. 2001), 2001.
[8] Y. Noda, H. Kon, Y. Furukawa, N. Otsuka, I. A. Nishida, K. Masumoto, Preparation and Thermoelectric Properties of $Mg_2Si_{1-x}Ge_x$ ($x = 0.0 \sim 0.4$) Solid Solution Semiconductors, Mater. Trans. 33 (1992) 845–850.
[9] E.N. Nikitin, V.G. Bazanov, V.I. Tarasov, Thermoelectric properties of solid solutions Mg_2Si-Mg_2Sn, Sov. Phys. Solid. State. 3 (1962) 2648–2651.
[10] H. Wang, H. Jin, W. Chu, Y. Guo, Thermodynamic properties of Mg_2Si and Mg_2Ge investigated by first principles method, J. Alloy. Compd. 499 (2010) 68–74.
[11] J. Tani, H. Kido, Thermoelectric properties of Bi-doped Mg_2Si semiconductors, Phys. B. Cond. Matter. 364 (2005) 218–224.
[12] H.J. Lee, Y.R. Cho, I.H. Kim, Synthesis of thermoelectric Mg_2Si by a solid state reaction, J. Ceram. Process. Res. 12(1) (2011) 16–20.
[13] K. Kawamura, K. Hirako, Material design using personal computer, Shokabo, Tokyo, 1994.
[14] S. Nose, A unified formulation of the constant temperature molecular dynamics methods, J. Chem. Phys. 81 (1984) 511–519.
[15] H.C. Andersen, Molecular dynamics simulations at constant pressure and/or temperature, J. Chem. Phys. 72 (1980) 2384–2393.
[16] P.M. Morse, Diatomic molecules according to the wave mechanics. II. Vibrational levels, Phys. Rev. 34 (1929) 57.
[17] Y. Ida, Interionic repulsive force and compressibility of ions, Phys. Earth Planet. Interiors. 13 (1976) 97–104.
[18] K.A. Bol'shakov, N.A. Bul'onkov, L.N. Rastorguev, M.S. Tairlin, Translated from Zhurnal Neorgranicheskoi. Khimii, Russ. J. Inorg. Chem. 8(12) (1963) 1418–1421.
[19] D. Chen, F. Peng, B. Yu, Periodic DFT study on the structural and thermal properties of bulk anti-fluorite magnesium silicide, Acta Metall. Sin. (Engl. Lett.). 24(4) (2011) 271–280.
[20] R. Zwanzig, Time-correlation functions and transport coefficients in statistical mechanics, Ann. Rev. Phys. Chem. 16 (1965) 67–102.
[21] J.Y. Jung, I.H. Kim, Synthesis of thermoelectric Mg_2Si by mechanical alloying, J. Kor. Phys. Soc. 57(4) (2010) 1005–1009.
[22] S.W. You, I. Kim, Solid-state synthesis and thermoelectric properties of Bi-doped Mg_2Si compounds, Curr. Appl. Phys. 11 (2011) S392–S395.
[23] K. Kim, S. Choi, W. Seo, Synthesis characteristics and thermoelectric properties of the rare-earth-doped Mg_2Si system, J. Kor. Phys. Soc. 57(4) (2010) 1072–1076.
[24] X. Hu, D. Mayson, M. Barnett, Synthesis of Mg_2Si for thermoelectric applications using magnesium alloy and spark plasma sintering, J. Alloy. Compd. 589 (2014) 485–490.
[25] T. Sakamoto, T. Iida, N. Fukushima, Y. Honda, M. Tada, Y. Taguchi, Y. Mito, H. Taguchi, Y. Takanashi, Thermoelectric properties and power generation characteristics of sintered undoped n-type Mg_2Si, Thin. Solid. Films. 519 (2011) 8528–8531.
[26] Y. Hayatsu, T. Iida, T. Sakamoto, S. Kurosaki, K. Nishio, Y. Kogo, Y. Takanashi, Fabrication of large sintered pellets of Sb-doped n-type Mg_2Si using a plasma activated sintering method, J. Sol. State Chem. 193 (2012) 161–165.
[27] Q.S. Meng, W.H. Fana, R.X. Chena and Z.A. Munir, Thermoelectric properties of Sc-and Y-doped Mg_2Si prepared by field-activated and pressure-assisted reactive sintering, J. Alloy. Compd. 509 (2011) 7922–7926.